Title: Histological scoring of immune and stromal features in breast and axillary lymph nodes is prognostic for distant metastasis in lymph node-positive breast cancers

Running title: Prognostic value of histological immune and stromal features

List of authors: Anita Grigoriadis[1,2,3*$], Patrycja Gazinska[1,2*], Trupti Pai [2,3,4], Sheeba Irhsad[1,2], Yin Wu[1,5], Rosemary Millis[2], Kalnisha Naidoo[6], Julie Owen[2], Cheryl E Gillett[2], Andrew Tutt[1,2,6], Anthonius CC Coolen[7], Sarah E Pinder[2]

* contributed equally

Full affiliations of all authors

[1] Breast Cancer Now Research Unit, Innovation Hub, Cancer Centre at Guy's Hospital, King's College London, Faculty of Life Sciences and Medicine, London SE1 9RT, UK.

[2] School of Cancer Studies, CRUK King's Health Partners Centre, King's College London, Innovation Hub, Cancer Centre at Guy's Hospital, Great Maze Pond, London SE1 9RT, UK.

[3] Cancer Bioinformatics, King's College London, Innovation Hub, Cancer Centre at Guy's Hospital, Great Maze Pond, London SE1 9RT, UK.

[4] Department of Pathology, Tata Memorial Centre, Tata, Memorial Hospital, 8th Floor, Annexe Building, Mumbai, India

[5] Peter Gorer Department of Immunobiology, King's College London, 2nd Floor, Borough Wing, Guy's Hospital, London, SE1 9RT, UK.

[6] Breast Cancer Now, The Institute of Cancer Research, London SW3 6JB, UK.

[7] Institute for Mathematical and Molecular Biomedicine, King's College London, Hodgkin Building, Guy's Campus, London SE1 1UL, UK.

$ corresponding author: anita.grigoriadis@kcl.ac.uk

Anita Grigoriadis

Cancer Bioinformatics, King's College London, Innovation Hub, Cancer Centre at Guy's Hospital, Great Maze Pond, London SE1 9RT, UK.

A conflict of interest statement

All authors declare no conflicts of interest.

A word count for the main text 3989/ 4000 words

ABSTRACT (298/300 words)

The prognostic importance of lymph node status and tumour infiltrating lymphocytes (TILs), is well established, particularly TILs in triple negative breast cancers (TNBCs). So far, few studies have interrogated changes in involved and uninvolved lymph nodes (LNs) and evaluated if their morphological patterns add valuable information for the prediction of disease progression in breast cancer.

In a cohort of 309 patients enriched for TNBCs (170/309), we histologically characterised immune and stromal features in primary tumours and associated involved and uninvolved axillary LNs on routine haematoxylin and eosin stained sections. Out of the 309 patients, 143 had LN-positive disease. Twenty-five histopathological features were assessed, including the degree of TIL presence, quantitative and qualitative assessment of germinal centres (GCs) and sinus histiocytosis. Multivariate and cross-validated proportional hazard regression analyses were used to identify optimal covariate sets for prediction of distant metastasis free survival (DMFS).

The degree of intratumoural and peritumoural immune infiltrate was associated with architectural changes in both uninvolved and involved LNs. By including clinicopathological characteristics as well as tumour and LN histopathological features in L2-regularised proportional hazard models, the prediction of 5-year DMFS was improved by 3-15% over the baseline in all cancers and in TNBCs. In LN-positive cancers, the combination of Salgado's classification, lymphocytic lobulitis, size and number of GCs in the uninvolved LN and location of GCs in the involved LN carried significant prognostic information. From these features, a multivariate cross-validation-stable risk signature was constructed, which identified low-risk groups within both LN-positive breast cancers and the LN-positive TNBCs group with a 10-year DMFS probability of 78% and 87%, respectively.

This study illustrates that by incorporating histopathological patterns of involved and uninvolved LNs combined with immune and stromal features of primary tumour, the prediction of developing distant metastasis in LN-positive breast cancers can be estimated more accurately.

Keywords: (3-10) immune and stromal tumour-environment, multivariate distant metastasis free survival analysis, lymph nodes, triple negative breast cancers, lymph node positive breast cancer.

INTRODUCTION

In invasive breast cancer, tumour size and the number of involved lymph nodes (LNs) have an inverse linear relationship with prognosis [1] and guide clinical decisions. Historical ten-year survival after local therapy alone (surgery and radiotherapy) in patients with node negative disease is ~85%, whilst for patients with involved axillary LNs it is 40-50% [2]. Emerging data has identified patients with a low risk for recurrence amongst LN-positive breast cancers who may be spared aggressive treatments. LNs are classified as involved with metastasis by pathological examination of conventional haematoxylin and eosin (H&E) sections, depending on the number of cancerous cells and size of the largest malignant deposit [3]. However, controversy regarding thresholds for these variables in addition to results from recent clinical trials in which occult metastasis were retrospectively evaluated [4], illustrate the uncertainty around the prognostic LN features on disease recurrence.

Accumulating evidence supports the prognostic and predictive role of the host immune response in early stage breast cancers, especially in oestrogen receptor (ER)-negative, progesterone receptor (PR)-negative and HER2-negative (i.e. triple negative) breast cancers (TNBCs) [5-7]. Recent studies have shown that stromal tumour infiltrating lymphocytes (TILs), as opposed to intratumoural TILs, are potentially useful biomarkers in predicting response to therapy and overall outcome, when assessed via light microscopy of H&E-stained tissue [5,8,9]. Most studies to date have focused on the assessment of TILs within the primary tumour whilst largely ignoring peritumoural and nodal patterns of immune infiltrates. Clinical relevance of cell type specific alteration in LNs was provided by Khort *et al*., who demonstrated that the number of CD4 T cells and CD1a dendritic cells in axillary LNs allowed a more significant stratification of disease-free survival for 77 breast cancer patients with small and medium-sized tumours than all other clinico-pathological features [10].

The aim of this study was (i) to comprehensively catalogue the histopathological features of immune cell and other mesenchymal stromal infiltrates within tumour tissue, peritumoural tissue and axillary nodal tissue and (ii) to determine whether any of these features are of prognostic value in breast cancer. Given the large number of features evaluated in relation to the small-sized patient cohorts, we implemented an L2-regularised multivariate Cox proportional hazard model with repeated cross-validation to identify robust and generalisable putative predictors of developing distant metastasis.

MATERIALS AND METHODS

Study design and patients

This is a retrospective study of patients with invasive breast carcinoma treated between 1984 to 2002 at Guy's Hospital London, UK. Ethical clearance was obtained from the local research ethics committee. H&E stained sections of formalin fixed paraffin embedded (FFPE) tissue from primary invasive breast carcinomas, along with their involved and uninvolved LNs, were retrieved from the King's Health Partner's Breast Cancer Tissue and Data Bank (London, UK) from 309 patients. The cohort was enriched for TNBCs patients with an N of 170 (142 of which were described previously [11]), whilst 139 patients had non-TNBC (hormone receptor-positive/HER2-negative (N=62), hormone receptor-negative/HER2-positive (N=59) and hormone receptor-positive/HER2-positive (N=18)). LN status was available for 276/309 patients. 143 (52%) patients were LN-positive whilst 133 (48%) had LN-negative disease. Uninvolved axillary LNs were available for 134/143 patients with LN-positive disease. In the remaining nine LN-positive patients, all harvested nodes were involved. Clinicopathological data for each patient, including age at diagnosis, baseline tumour characteristics such as invasive size, histological grade, histological subtype, ER, PR and HER2 status, and immunohistochemistry (IHC)) for cytokeratins (CK) 5 and 14 and epidermal growth factor receptors (EGFR) status, LN involvement and distant metastases were recorded (Table 1) and some have previously been described [11].

Histopathological immune assessment:

Classification of immune infiltrates

All routine H&E stained sections of primary breast tumours and uninvolved and involved LNs were reassessed histopathologically. A minimum of 6 sections of the primary tumour and 1-12 (mean=6) LNs per case were available for evaluation of immune and stromal features. All sections were reviewed by a specialist Consultant Breast Pathologist (SEP) and Pathology Research Scientist (PG). Analyses of the tumour microenvironment were performed using conventional microscopy of H&E whole sections. The NanoZoomer HT Digital Pathology Scanning System (Hamamatsu, Japan), was used to scan H&E sections with a spatial resolution of 0.46 µm/pixel for the measurement of LN germinal centres (GCs). According to recommendations by the International Tumour Infiltrating Lymphocytes Working Group [12], morphological features initially assessed as continuous variables (*e.g.* stromal TILs) were discretised for statistical analysis. All features and their associated categories described below in detail are summarised in Supplementary Table S1A & S1B.

Intratumoural site:

Immune infiltrates were assessed semi-quantitatively across the entire tumour section and then in different tumour regions. As per Salgado's criteria, TILs were classified as 'stromal TILs' (Figure 1A-C) or 'intratumoural TILs' (Figure 1D). Stromal TILs were further subclassified as TILs scattered within the tumour stroma (Figure 1A); TILs around tumour cell nests (Figure 1B) and TILs seen at the invasive margin (Figure 1C). The degree of TILs present was further graded semi-quantitatively as: 0=absence of lymphocytes, 1=minimal (1 - 10% of surface area in a given location); 2=mild (10 - 20%); 3=moderate (>20 - 50%); and 4=strong (≥50%).

Peritumoural site (including premalignant and non-tumorous components):

Immune infiltrates in situ and normal tissue adjacent to invasive tumours were assessed when seen (i) next to DCIS (Figure 1E), (ii) in normal breast lobules

(Figure 1F), and (iii) in perivascular areas (Figure 1G). Lymphocytic lobulitis ([13](Figure 1H) and tertiary lymphoid structures (TLS) were graded as present or absent (Figure 1I).

Stromal features:

Assessment of stromal features in the invasive tumours was based on their overall appearances and recorded as oedematous/myxoid (Figure 1J), hyalinised (Figure 1K) and/or fibroblastic (Figure 1L); when a mixed pattern was present, the predominant feature was recorded. Smooth muscle actin (SMA) and alcian blue staining of selected cases supported the H&E stromal classification (Supplementary Figure S1).

Involved and uninvolved axillary LNs

Three main morphological immune features were assessed in axillary involved LNs: A) Germinal centre features, B) Degree of sinus histiocytosis and C) Pattern of metastatic tumour involvement (Supplementary Table S1B). In uninvolved LN, only A) and B) were assessed:

(i) The number of GCs was categorised as grade 0 (absent), 1 (few), 2 (moderate) or 3 (numerous, frequently distributed throughout the LN) (Figure 2 A). (ii) The distribution of GCs was classified as predominantly peripheral (majority close to the capsule), predominantly central (most GCs in the centre of the LN) (Figure 2A) or mixed architecture (GCs were located across the whole LN). (iii) Average size of GCs was classified as either small (< 200 µm in diameter), moderate (200-400 µm), large (> 400 µm) or mixed (if more than one size) (Figure 2B). In those with mixed sizes of GCs, cases with a predominant pattern of large GCs, were further classified as “GC hyperplasia”. Supplementary Figure S2 shows staining CD20 (B cell marker) and CD11c (dendritic cell marker) on selected cases, which corroborated the classification of morphological changes in the germinal centres of the LNs.

Sinus histiocytosis was assessed using a modification of the method previously described by Culter *et al.* [14]. The number of histiocytes across the sinuses was classified as: grade 0 (absent), grade 1 (<2 cells), grade 2 (2-

4 cells), grade 3 (>4-<8 cells) or grade 4 (≥8 cells across the sinus) (Figure 2C). The dilatation of sinuses by cells other than histiocytes, for example by metastatic tumour cells, or other inflammatory cells or oedema fluid, was ignored.

The metastatic tumour spread within the LN was classified into six patterns: i) sub-capsular (within the sinus immediately under the LN capsule) (Figure 2D), ii) intra-sinusoidal (within sinuses in the body of the LN (Figure 2E), iii) diffuse (Figure 2F), iv) nodular (Figure 2G), v) mixed (mixture of several patterns) and vi) total replacement by tumour.

Data analysis and interpretation

The end point of the study was distant metastasis free survival (DMFS), which was calculated from the date of diagnosis of the primary tumour to the first event of any distant metastases. An L2-regularised multivariate proportional hazard model, based on iterative determination of optimal covariates to prevent overfitting via repeated cross-validation, was applied to all breast cancers (N=309), TNBC (N=170) patients, and their LN-status dichotomised subgroups [15-18]. Three sets of covariates were used in the analytical models: group A included 8 clinico-pathological features, group B encompassed histologically assessed immune and stromal features and group C was a combination of A and B. Figure 3 provides a CONSORT diagram explaining cohorts used for statistical analyses. A detailed description of the statistical analysis is provided in Supplementary Method and Supplementary Figure S3. In brief, each analysis was performed with 100 iterations and their results were averaged. The fraction of correctly predicted patients was recorded after 1 year, and every year up to 10 years of DMFS. At each time point, an optimal set of covariates with the highest prediction accuracy was determined by ranking the covariates according to their relevance in the cross-validated Cox regression analysis. Regression parameters for each covariate were reported as hazard ratios (HR) with 95% confidence intervals (CI) [19].

For LN-positive cohorts, an optimal covariate-set to predict 5-year DMFS was established to construct a single-patient immune and stromal histopathological (ISH)-risk score, by summing the standardised covariates weighted by their coefficients. LN-positive patients were grouped into those with low and upper quartile, and mean risk signature scores. Kaplan Meier estimators were used, and the log-rank test was performed to test differences among groups.

RESULTS

Clinicopathological characteristics of the patients

The clinicopathological features of the 309 evaluated patients are presented in Table 1. First analysis was restricted to TNBC patients (N=170, 81 with LN-negative and 64 with LN-positive disease and 25 patients within unknown LN-status), followed by randomly selected non-TNBC patients (N=139; 52 with LN-negative, 79 LN-positive and 8 with unknown LN status). All patients were female with a median age of 55 years (range=24-89) at diagnosis. Most (N=183; 59%) patients had T2 tumour size and a predominant number of cases (N=253; 82%) were histologically grade 3, as might be expected in a cohort enriched for TNBC and for LN positive cases. Most cases were invasive breast carcinomas of no special type (82%). Lymphovascular invasion (LVI) was seen in 90 (29%) cases. Median follow-up was 7.9 years for the entire cohort (range=0.3-25). Distant metastasis was recorded in 129 (42%) patients, of whom 70% developed distant metastasis within the first 2.5 years after diagnosis (range of DMFS 0.3-18 years).

Lymphocytic infiltration at invasive and peritumoural sites

Intratumoural sites:

An absence of lymphocytic infiltration across the entire tumour was noted in 6 (3.5%) TNBC patients compared with 18 (12.9%) non-TNBC patients. The majority of TNBC patients had a moderate (N=78, 45.9%) or strong (N=23, 13.5%) degree of lymphocytic infiltration across the entire tumour. In contrast, a majority of non-TNBC patients had minimal (N=45, 32.4%) or mild (N=36, 25.9%) degree of infiltration. A strong degree of lymphocytic infiltration across the entire tumour was seen only in 5 (3.6%) non-TNBC patients. Intratumoral

TILs were present in more TNBC patients (N=51, 30%) compared with non-TNBC patients (N=10, 7.2%). Likewise, a strong degree of TILs at the invasive margins was noted in more TNBC (N=22, 12.9%) than non-TNBC patients (N=2, 1.4%).

Peritumoural sites

In 130 of the total 309 cases, DCIS was seen in close proximity to the invasive tumour. In 48/130 (36.9%) cases, the DCIS was free of lymphoid infiltrate, whilst the rest had varying degrees of immune infiltrates. A strong lymphoid infiltrate was found surrounding breast lobules in the TNBC group (N=40, 30.5%) compared with the non-TNBC group (N=20, 17.5%). Lymphocytic lobulitis and TLS in areas surrounding the invasive tumours were seen more frequently in TNBC cases (16% and 27.6%, respectively) compared with non-TNBCs, (9.6% and 17.3%, respectively).

Tumour stroma

Fibroblastic stroma was the most common intratumoural stromal change noted accounting for 87% cases, followed by hyalinised stroma in 86% cases and myxoid change was the least common noted in 23% cases. No differences were noted across tumour subgroups (Table 2B).

Histological evaluation of involved and uninvolved axillary lymph nodes

Primary tumours may lead to reactive and structural changes in regional lymph nodes prior to development of nodal metastases [20,21]. A total of 267 uninvolved and 143 involved lymph nodes were reviewed. GCs were present in 193 uninvolved lymph nodes (72%), and 97 involved lymph nodes (67%) and assessed for their number, location and size. Within involved lymph nodes, GCs were located mainly in the periphery (52.6%) or predominantly in the centre of LNs (21.6%) (Table 2C). The numbers of large GCs, and the overall size distribution in uninvolved and involved LN was comparable (Table 2C). Similarly, the frequency of grade 3-4 sinus histiocytosis was comparable.

Correlation of histopathological features of intratumoural, peritumoural, stromal and nodal sites

We next investigated whether the degree and presence of these histological features occurred independently. Using a Pearson's correlation, there was a concurrent increase in the degree of lymphocytic infiltrate at the invasive tumour, around tumour nests, at the peripheral tumour edge and within the stroma (Supplementary Figure S4). We also noticed that in all breast cancers and particularly among TNBCs, the number and size of the GCs in uninvolved and involved lymph nodes grew with increasing levels of immune infiltrates at the primary tumour site (r: 0.46, $P < 0.001$; Supplementary Figure S4).

Immune-associated characteristics improve prognostic accuracy of DMFS

Next, we asked whether these novel histomorphological features carry prognostic information for the development of distant metastases. Given that several of these immune and stroma cell patterns do not occur independently (Supplementary Figure S4), we used a Bayesian multivariate survival analysis algorithm optimised to undo the possible effects of overfitting [18]. We analysed three groups of covariates (A, B, C) first in all breast cancers and then in the TNBC cohort only. We then evaluated their performance in correctly predicting the fraction of patients free of distant metastasis at 5 years after diagnosis in comparison to the baseline performance in which no covariates were used and in which the risk of distant metastasis is derived solely on any imbalance between cases and controls (Figure 4, vertical grey line). Covariate-group A included 8 clinicopathological features; ER, PR and HER2 status, histological grade, lymph node status, tumour size, age at diagnosis and the presence or absence of LVI. Group B encompassed the 25 histologically assessed features described above in detail (14 features are from the primary tumour site and 11 features were obtained from involved and uninvolved LNs, Supplementary Table 1). In group C, we combined groups A and B. In all breast cancers, covariate-group A correctly predicted 5-year DMFS in 68% of patients (green lines, Figure 4A). This was a modest improvement compared to 62% baseline performance (dotted line, Figure 4A) and the covariate-group B (red line, Figure 4A). The combined covariate-group C performed best by correctly predicting 5-year DMFS in 71% of patients (black line, Figure 4A). In TNBC, the differences in predictive accuracy between groups A, B and C were less pronounced. Of note, within the TNBC cohort, covariate-group B (red line, Figure 4B) was more accurate in predicting 5-year DMFS (71%) than either group A (67%, green line, Figure 4B) or the baseline performance (67%, dotted line, Figure 4B). The optimal covariates among the covariate-group B were selected as being risk-predictive at 5-year DMFS, namely TILs in the primary tumour according to Salgado's criteria [12], the number and size of GCs in the uninvolved LN, the location of GCs and a diffuse metastatic pattern in the involved LN, as well as the presence of lymphocytic lobulitis in adjacent normal breast tissue (Table 3). Supplementary Table 2A provides the full list of optimal covariates selected at 5-year DMFS in both cohorts for each of the three covariate-groups used in these analyses.

A risk score based on histomorphological features identifies LN-positive breast cancers patients with low risk for distant metastasis

Since morphological patterns in involved and uninvolved LNs carried prognostic value, we asked if these features were predictive for developing distant metastasis in both LN-positive and LN-negative disease. All breast cancers and TNBCs group were further divided into patients with LN-positive (143 all cancers and 64 TNBC), and LN-negative disease (133 all cancers and 81 TNBC). These four sub-cohorts were then analysed independently with L2-regularised proportional hazards models using covariate-group B. In the LN-positive cohorts, covariates were selected via cross-validation for predicting a 5-year DMFS, including Salgado's classification, the presence of lymphocytic lobulitis, the size and number of GCs in the uninvolved LN and location of GCs in the involved LN (Table 3, Supplementary Table 2B and 2C). Incorporating these five features improved the 5-year DMFS predictive accuracy from 50% baseline performance (dotted line, Figure 4C) to 64% in all breast cancers (red line, Figure 4C) and from 58% baseline performance (dotted line, Figure 4D) to

73% in TNBC (red line, Figure 4D). Amongst the two LN-negative cohorts, covariate-group B failed to improve 5-year DMFS predictive accuracy (Supplementary Figure S5). Due to the smaller datasets in these sub-cohorts, residual overfitting cannot be excluded.

Lastly, we built an “immune-stroma-histological (ISH)-risk score” with these 5 histomorphological features (see Supplementary Method), and grouped patients according to their ISH-risk score levels. Patients with the lowest quartile ISH-risk scores had a 10-year DMFS of 78% (all breast cancer cohort) and 87% (TNBC cohort) compared with 17% (all breast cancer cohort) and 18% (TNBC cohort) for patients with an upper quartile ISH-risk score (Kaplan Meier survival estimates; log-rank test of difference in survival, $p < 0.001$, HR = 5.15, 95% CI 3.8–6.97; $p < 0.001$, HR = 14.26, 95% CI 7.48–27.19) (Figure 4E & F). Moreover, LN-positive breast cancer patients with low ISH-risk score had even less risk of developing distant metastases than LN-negative breast cancer patients (Figure 4E & F, black dotted line). This suggests that histomorphological changes within uninvolved and involved LN carry significant prognostic information for the risk of distant metastasis amongst LN-positive patients, even among triple negative breast cancers.

DISCUSSION

It is well known that routinely assessable clinicopathological characteristics such as LN status or the presence of TILs predict the risk of recurrence, distant metastases and overall outcome in breast cancer patients. In this study, we have utilised an optimised multivariate proportional hazard model for analysing ‘time-to-event’ data which was based on extensive H&E histopathological data to determine whether these features are of prognostic value in breast cancer. Reassuringly, well-established prognostic markers were shown to be associated with outcome, including the presence of LN metastases whilst we also confirm the value of the Salgado classification [12]. We report, for the first time, that the number and architecture of GCs in involved and uninvolved LNs, as well as the presence of lymphocytic lobulitis, provide important information for outcome prediction. Selected through L2-regularised and cross-validated proportional hazards models, we have developed a novel risk score, identifying patients with low risk for developing metastases even amongst patients with LN-positive breast cancers.

There is now increasing interest in the role of the tumour microenvironment in cancer prognosis and, in particular, the role of lymphocytic infiltrates and stromal reactions. TIL composition within the primary invasive tumour has proven to be superior to the classical TNM staging in predicting outcome in some series [12]. TIL composition has also been shown to be predictive of response to chemotherapeutic agents [8,20-22]. Much of this, however, relies on complex multi-parametric surface phenotyping of TILs from fresh frozen or freshly dissociated tissues. Unsurprisingly, given the technical challenges, financial constraints and operator dependence, these immune scoring systems have not been widely adopted in routine clinical practice despite their potential benefits. Our work provides a novel scoring system that can accurately predict DMFS, particularly in LN-positive and triple negative breast cancers, based on routine H&E histopathological examination. Hence, unlike complex multi-parametric assays, our method could be easily integrated into standard clinical practice.

To our knowledge, we are the first to include the histological features of uninvolved LNs into a predictive model of DMFS for breast cancer patients. Although draining LNs are the first site of metastasis for many cancers, the histological progression from an uninvolved to an involved LN remains poorly documented. A recent study in murine models found that the stromal compartments in uninvolved LNs undergo structural reorganisation due to the proliferation and transcriptional changes of fibroblastic reticular cells, potentially providing a pro-tumour environment [22]. While we cannot attribute changes to specific cell types within the uninvolved LNs, we observed in this study that patients with shorter time to any distant metastasis had fewer and larger GCs, which were predominantly located in the centre of the node. GCs are dynamic structures where B cells expressing high-affinity, potentially tumour-reactive antibodies mature into antibody-secreting plasma cells and memory B cells. Further studies are clearly warranted to elucidate molecular signals in uninvolved LNs that may predict development of nodal metastases.

The presence of lymphocytic lobulitis adjacent to the primary tumour was another feature associated with a reduced risk of recurrence in all breast cancers and TNBCs, including LN-positive cohorts. Lymphocytic lobulitis is characterised by perilobular and perivascular aggregates of B and T lymphocytes with increased expression of MHC class II antigens by the lobular and ductal epithelium and has been described in prophylactic mastectomies from women with *BRCA1*/2 mutations [23]. In normal breast tissue, immune cells are predominantly localised to lobules. In lymphocytic lobulitis, disproportionately higher numbers of T cells (CD4 and CD8) and B cells (CD20) are seen when compared with dendritic cells or monocytes/macrophages. The role of these cells in the breast is not entirely clear, although a role in tissue immune surveillance has been proposed [24].

Through incorporating the variability of immune and stromal composition at the primary tumour bed, along with architectural changes in uninvolved and involved LNs, we were able to develop an ISH-risk score to identify low-risk patients among LN-positive breast cancers. Effective biomarkers to guide clinical management is of particular importance in high-risk patients such as those with TNBC and LN-positive disease. These patients are often referred for adjuvant chemotherapy but only a proportion benefit from increased overall survival. Currently there is a lack of validated biomarkers to identify patients for whom less aggressive intervention might be appropriate. Our ISH-risk score was derived through an unbiased approach, in which we aimed to: (1) quantify the outcome prediction performance of regression results; (2) avoid overfitting via monitoring of outcome prediction on unseen data, and; (3) construct a multivariate risk signature based on the optimised covariate set. Thus, we propose that our

ISH-risk score might be used for effective patient stratification, although clearly this requires further evaluation.

This study has several limitations. Firstly, the breast cancer cohort used was enriched for TNBCs (170/309) which frequently have increased immune infiltrates compared with other subtypes of breast cancer. Thus, future studies in cohorts with higher proportions of ER-positive or HER2-positive breast cancers are warranted to corroborate the applicability of these histomorphological features. Secondly, as a high proportion of tumours, particularly TNBCs, were of histological grade 3, this pathological characteristic was non-discriminatory for risk prediction in this cohort. In cohorts with more typical distribution of histological grade of consecutive series of invasive breast cancers, the inclusion of histological grade in the multivariate model will need to be evaluated. Finally, we have not as yet sub-categorised immune and stromal cells in uninvolved LNs, particularly in the GCs, with orthogonal experiments such as IHC or immunofluorescence techniques. Although this would shed further light on the pro-tumour evolving microenvironment in these lymphoid organs, they are beyond the scope of this manuscript.

In conclusion, our study highlights the added value of comprehensive histopathological examination of tumoural, peritumoural and nodal features for the prediction of distant metastases. By suppressing overfitting via repeated cross-validation and constructing reproducible multivariate risk signatures, our mathematical approach provides a robust method for survival analysis beyond the commonly used Kaplan Meier analyses. Furthermore, these results point towards a novel histopathological prognostic tool that improves 5-year DMFS prediction accuracy in high-risk breast cancers and if validated, could be implemented in standard histological practice.

Acknowledgements:

Patient samples and data were provided by King’s Health Partners Cancer Biobank, which is supported by the Department of Health via the National Institute for Health Research (NIHR) comprehensive Biomedical Research Centre award and the Experimental Cancer Centre at King’s College London. We thank Professor Agamemnon Grigoriadis for helping with the figures. PG, SI, AG and AT were supported by Breast Cancer Now Unit (former known as Breakthrough Breast Cancer Research) funding at King's College London and by the National Institute for Health Research Biomedical Research Centre based at Guy's and St Thomas' NHS Foundation Trust and King's College London.

Statement of author contributions

Concept and design: AG, PG, AT, SP. Data acquisition: PG, AG, JO, CG, AT, SP. Data analysis and interpretation: AG, PG, TP, ACCC, KN, YW, AT, SP. Wrote the manuscript: AG, PG, TP, SI, RM, YW, AT, ACCC, SP. Critically reviewed the manuscript: AG, PG, ACCC, TP, SI, KN, YW, AT, SP.

REFERENCES

1. Carter CL, Allen C, Henson DE. Relation of tumor size, lymph node status, and survival in 24,740 breast cancer cases. *Cancer* 1989; **63**: 181-187.
2. Early Breast Cancer Trialists' Collaborative Group, McGale P, Taylor C*, et al.* Effect of radiotherapy after mastectomy and axillary surgery on 10-year recurrence and 20-year breast cancer mortality: meta-analysis of individual patient data for 8135 women in 22 randomised trials. *Lancet* 2014; **383**: 2127-2135.
3. Edge SB, Compton CC. The American Joint Committee on Cancer: the 7th edition of the AJCC cancer staging manual and the future of TNM. *Annals of surgical oncology* 2010; **17**: 1471-1474.
4. Weaver DL, Ashikaga T, Krag DN*, et al.* Effect of occult metastases on survival in node-negative breast cancer. *The New England journal of medicine* 2011; **364**: 412-421.
5. Denkert C, Loibl S, Noske A*, et al.* Tumor-associated lymphocytes as an independent predictor of response to neoadjuvant chemotherapy in breast cancer. *Journal of clinical oncology : official journal of the American Society of Clinical Oncology* 2010; **28**: 105-113.
6. Irshad S, Grigoriadis A, Lawler K*, et al.* Profiling the immune stromal interface in breast cancer and its potential for clinical impact. *Breast care* 2012; **7**: 273-280.
7. Loi S, Sirtaine N, Piette F*, et al.* Prognostic and predictive value of tumor-infiltrating lymphocytes in a phase III randomized adjuvant breast cancer trial in node-positive breast cancer comparing the addition of docetaxel to doxorubicin with doxorubicin-based chemotherapy: BIG 02-98. *Journal of clinical oncology : official journal of the American Society of Clinical Oncology* 2013; **31**: 860-867.
8. Denkert C, von Minckwitz G, Brase JC*, et al.* Tumor-infiltrating lymphocytes and response to neoadjuvant chemotherapy with or without carboplatin in human epidermal growth factor receptor 2-positive and triple-negative primary breast cancers. *Journal of clinical*

oncology : official journal of the American Society of Clinical Oncology 2015; **33**: 983-991.

9. Gu-Trantien C, Willard-Gallo K. Tumor-infiltrating follicular helper T cells: The new kids on the block. *Oncoimmunology* 2013; **2**: e26066.
10. Kohrt HE, Nouri N, Nowels K*, et al.* Profile of immune cells in axillary lymph nodes predicts disease-free survival in breast cancer. *PLoS medicine* 2005; **2**: e284.
11. Gazinska P, Grigoriadis A, Brown JP*, et al.* Comparison of basal-like triple-negative breast cancer defined by morphology, immunohistochemistry and transcriptional profiles. *Modern pathology : an official journal of the United States and Canadian Academy of Pathology, Inc* 2013; **26**: 955-966.
12. Salgado R, Denkert C, Demaria S*, et al.* The evaluation of tumor-infiltrating lymphocytes (TILs) in breast cancer: recommendations by an International TILs Working Group 2014. *Annals of oncology : official journal of the European Society for Medical Oncology / ESMO* 2015; **26**: 259-271.
13. Gulbahce HE, Vanderwerf S, Blair C*, et al.* Lobulitis in nonneoplastic breast tissue from breast cancer patients: association with phenotypes that are common in hereditary breast cancer. *Human pathology* 2014; **45**: 78-84.
14. Culter SJ, Black MM, Goldenberg IS. Prognostic Factors in Cancer of the Female Breast. I. An Investigation of Some Interrelations. *Cancer* 1963; **16**: 1589-1597.
15. Fan JF, Yang; Wu, Yichao. . High-dimensional variable selection for Cox's proportional hazards model. Borrowing Strength: Theory Powering Applications – A Festschrift for Lawrence D. Brown. *Institute of Mathematical Statistics, Beachwood, Ohio, USA, 2010* 2010.
16. Moons KG, Donders AR, Steyerberg EW*, et al.* Penalized maximum likelihood estimation to directly adjust diagnostic and prognostic prediction models for overoptimism: a clinical example. *Journal of clinical epidemiology* 2004; **57**: 1262-1270.

17. Simon RM, Subramanian J, Li MC*, et al.* Using cross-validation to evaluate predictive accuracy of survival risk classifiers based on high-dimensional data. *Briefings in bioinformatics* 2011; **12**: 203-214.
18. Witten DM, Tibshirani R. Survival analysis with high-dimensional covariates. *Statistical methods in medical research* 2010; **19**: 29-51.
19. van Houwelingen HC, Bruinsma T, Hart AA*, et al.* Cross-validated Cox regression on microarray gene expression data. *Statistics in medicine* 2006; **25**: 3201-3216.
20. Loi S, Michiels S, Salgado R*, et al.* Tumor infiltrating lymphocytes are prognostic in triple negative breast cancer and predictive for trastuzumab benefit in early breast cancer: results from the FinHER trial. *Annals of oncology : official journal of the European Society for Medical Oncology / ESMO* 2014; **25**: 1544-1550.
21. Pruneri G, Gray KP, Vingiani A*, et al.* Tumor-infiltrating lymphocytes (TILs) are a powerful prognostic marker in patients with triple-negative breast cancer enrolled in the IBCSG phase III randomized clinical trial 22-00. *Breast cancer research and treatment* 2016; **158**: 323-331.
22. Riedel A, Shorthouse D, Haas L*, et al.* Tumor-induced stromal reprogramming drives lymph node transformation. *Nature immunology* 2016; **17**: 1118-1127.
23. Hermsen BB, von Mensdorff-Pouilly S, Fabry HF*, et al.* Lobulitis is a frequent finding in prophylactically removed breast tissue from women at hereditary high risk of breast cancer. *The Journal of pathology* 2005; **206**: 220-223.
24. Degnim AC, Brahmbhatt RD, Radisky DC*, et al.* Immune cell quantitation in normal breast tissue lobules with and without lobulitis. *Breast cancer research and treatment* 2014; **144**: 539-549.

TABLES

Table 1. Clinicopathological features of all breast cancers and TNBC

Table 2. A. Distribution of the immune features at tumoural and peri-tuoural sites assessed across TNBC and Non-TNBC subgroups. B. Distribution of the stromal features in TNBC and Non-TNBC subgroups. C: Pattern of histomorphological features in involved and uninvolved lymph nodes in LN-positive and LN-negative patients.

Table 3. Immune, stroma and lymph node feature selection from multivariate Bayesian Cox regression analyses. Features are listed and their hazard ratio shown if it was selected from group A (standard features), group B (immune & stroma features) and group C (all features). All cohorts that were used for analyses are reported. Covariates used for the Immuno-stroma -histological (ISH)-risk score are indicated in grey.

FIGURE LEGENDS

Figure 1: Morphological assessment of the immune parameters in the intratumoural and peritumoural sites of the primary tumour. (H&E stain).
(I) Intratumoural site:
(A) TILs scattered in the intratumoural stroma (score 4; ≥50%; strong); (B) TILs around tumour cell nests, (score 4; ≥50%; strong); (C) TILs at the invasive tumour margin (score 4; ≥50%; strong); (D) Presence of intratumoural TILs (lymphocytes present within tumour cell nests 'intra-epithelial').
(II) Peritumoural components:
(E) Lymphocytic infiltrate surrounding DCIS (score 3; ≥50%; strong); (F) Lymphocytic infiltrate surrounding normal breast lobules (score 3; ≥50%; strong); (G) Perivascular lymphocytic infiltrate (score 3; ≥50%; strong); (H) Presence of lymphocytic lobulitis (I) Presence of tertiary lymphoid structure (TLS) (lymphoid GC formation). Stromal features in the tumour environment: (J) oedematous/myxoid; (K) hyalinised stroma; (L) fibroblastic stroma.

Figure 2: Histomorphological features of uninvolved and involved lymph nodes (H&E stain)
In the uninvolved LNs: (A) numerous GCs (Grade 3) GC located throughout the LN (white arrows); (B) large GC (white arrow) with an adjacent small GC (black arrow); (C) sinus histiocytosis grade 4 (inset showing a higher power view). In the involved LNs: (D) supcapsular metastasis; (E) sinusoidal pattern (black arrows); (F) diffuse pattern (black arrows); (G) nodular pattern with near total replacement of the nodal tissue with metastatic deposits.

Figure 3: Consort diagram of cohorts used in the optimised multivariate proportional hazard model. A) 309 breast cancer and 170 TNBC patients were analysed with group A (standard features, big dashed box); group B (immune & stroma features, small dashed box) and group C (combination of standard and immune & stroma, plus additional 8 characteristics, black box). B) Stratification of cohorts into LN-positive and LN-negative patients.

Multivariate proportional hazard model was applied using group B features (immune & stroma features, small dashed box).

Figure 4: Optimised proportional hazards models to identify covariates for the prediction of developing distant metastasis in all invasive breast cancers and TNBC cohorts. Three different initial sets of covariates were used for the prediction analysis, namely 8 standard features (group A); 25 immune & stroma features (group B); and all available features in (group C). The dotted line in all graphs indicates the baseline performance without any covariates (i.e. based solely on any imbalance between cases and controls). The green, red and black, lines show the performance on the validation set including either group A, B and C, respectively. LN-positive patients of all breast cancers (C) and TNBC (D) were analysed with group B covariates. The LN-positive cohorts were further dichotomised based on the ISH-risk score. Kaplan Meier curves for all breast cancers (E) and TNBC (F) illustrating the duration of distant metastasis free survival (DMFS) according to lower quartile (green line), mean (blue line) and upper quartile (red line) of ISH-risk score grouping. Hazard ratio (HR), and confidence interval (CI) are listed below the graph. The black dotted lines display the survival curves for LN-negative patients of all breast cancers (N=133) and TNBC (N=81).

SUPPLEMENTARY DATA

Supplementary Table 1: Histopathological evaluation of primary tumour microenvironment (14 characteristics), uninvolved lymph nodes (5 characteristics), and involved lymph nodes (6 characteristics).

Supplementary Table 2: Results from multivariate L2-regularised and cross-validated proportional hazard analysis using group A, B and C of immune and stroma histomorphologically assessed and clinicopathological characteristics. Taken at the 5 year prediction cut off time point.

Supplementary Figure S1: Smooth muscle actin (SMA) and alcian blue staining of selected primary tumours with differing stromal features.

Supplementary Figure S2: Germinal centres of the LNs stained with CD20 (B cell marker) and CD11c (dendritic cell marker).

Supplementary Figure S3: Identification of overfitting point in the Bayesian batch Cox analysis. Graphs illustrating the fraction of correctly predicted disease outcome for patients (i.e. those who had an event prior the cut-off time) (prediction time point) over those patients who had either never distant metastasis or developed metastasis after this time point. The top and bottom lines represent the validation and test sets, respectively. The number of covariates used for the prediction is shown on the x-axis (*nr of covs*). Iteratively, covariates are removed from the analysis.

Supplementary Figure S4: Correlations analysis of covariates. Plot showing all pairwise Pearson's correlations for standard clinical features and all novel morphological assessed features across 309 breast carcinomas in (A) and for all histopathological characteristics across TNBC (B). The list of covariates is provided at the bottom, whereby immune-associated features are indicated in blue, features assessed in the uninvolved lymph node in purple, in the involved lymph node in green and standard clinic-pathological features in black. We also included the relevant outcome variable (TTE – time to event).

Supplementary Figure S5: Optimised proportional hazards models to identify covariates for the prediction of distant metastasis-free survival (DMFS) in all breast cancers LN-negative and TNBC LN-negative cohorts.

Supplementary Materials and methods: Detailed description of the L2-regularised and cross-validated proportional hazard analysis.

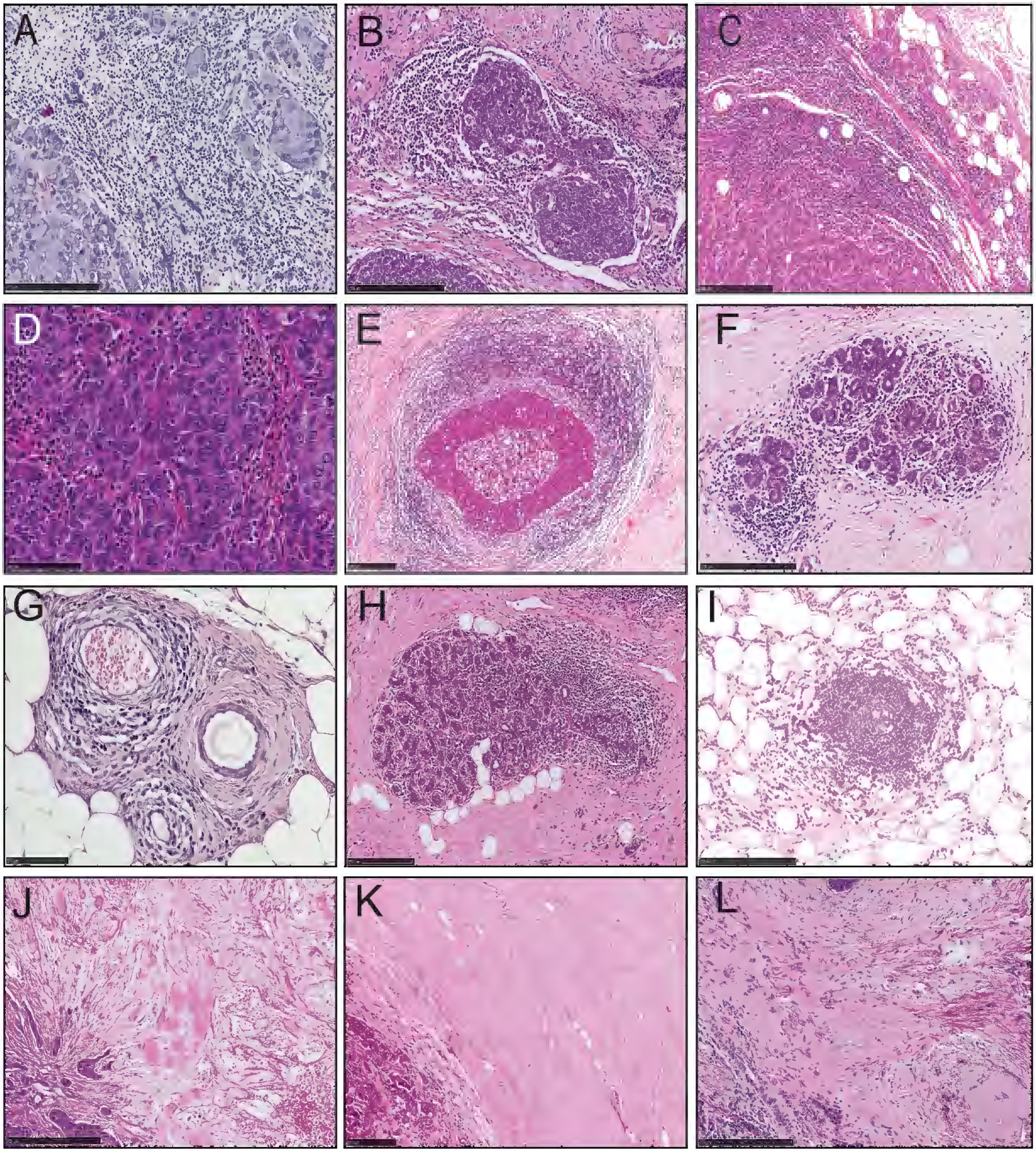
A
B
C
D
E
F
G
H
I
J
K
L

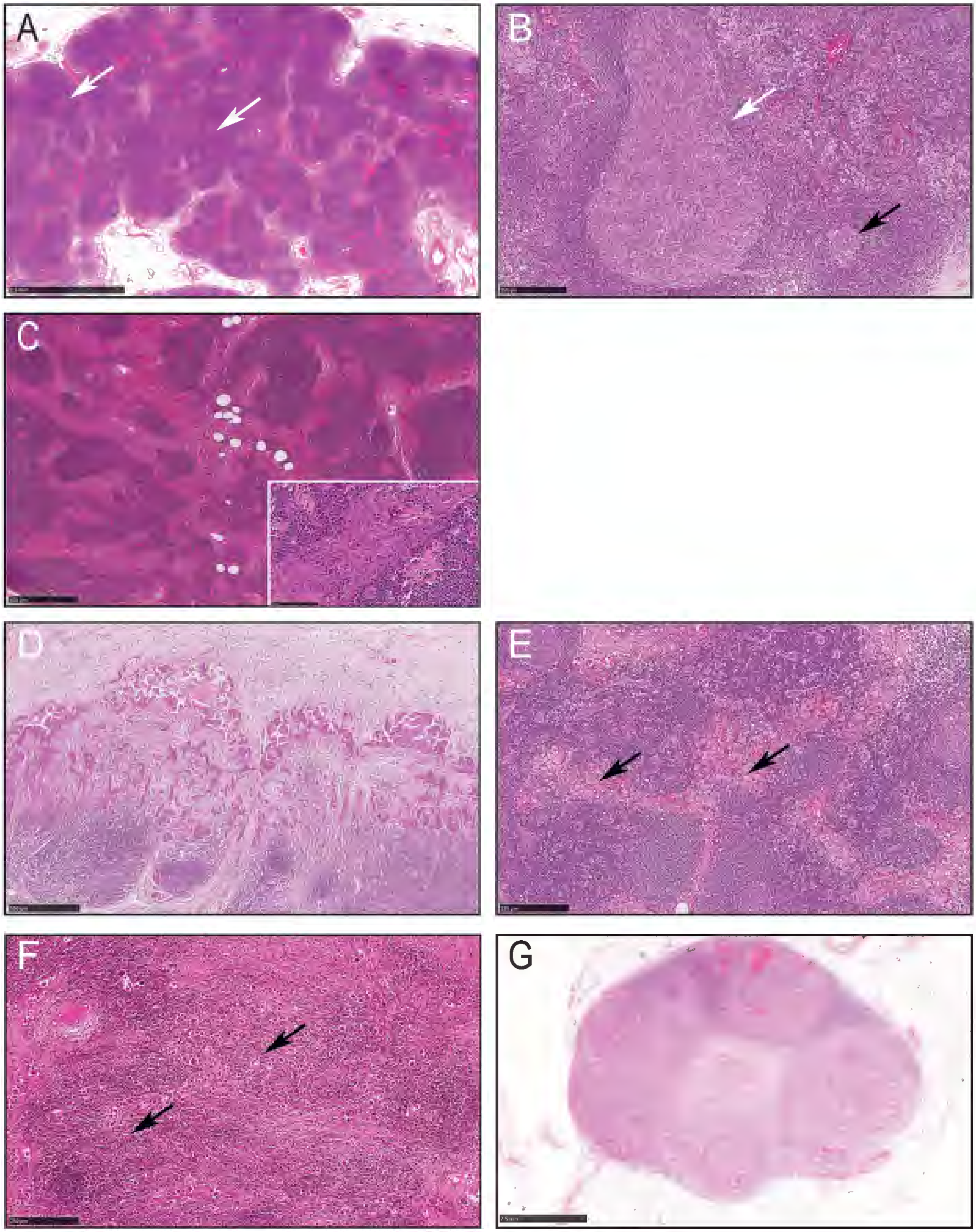
A
B
C
D
E
F
G

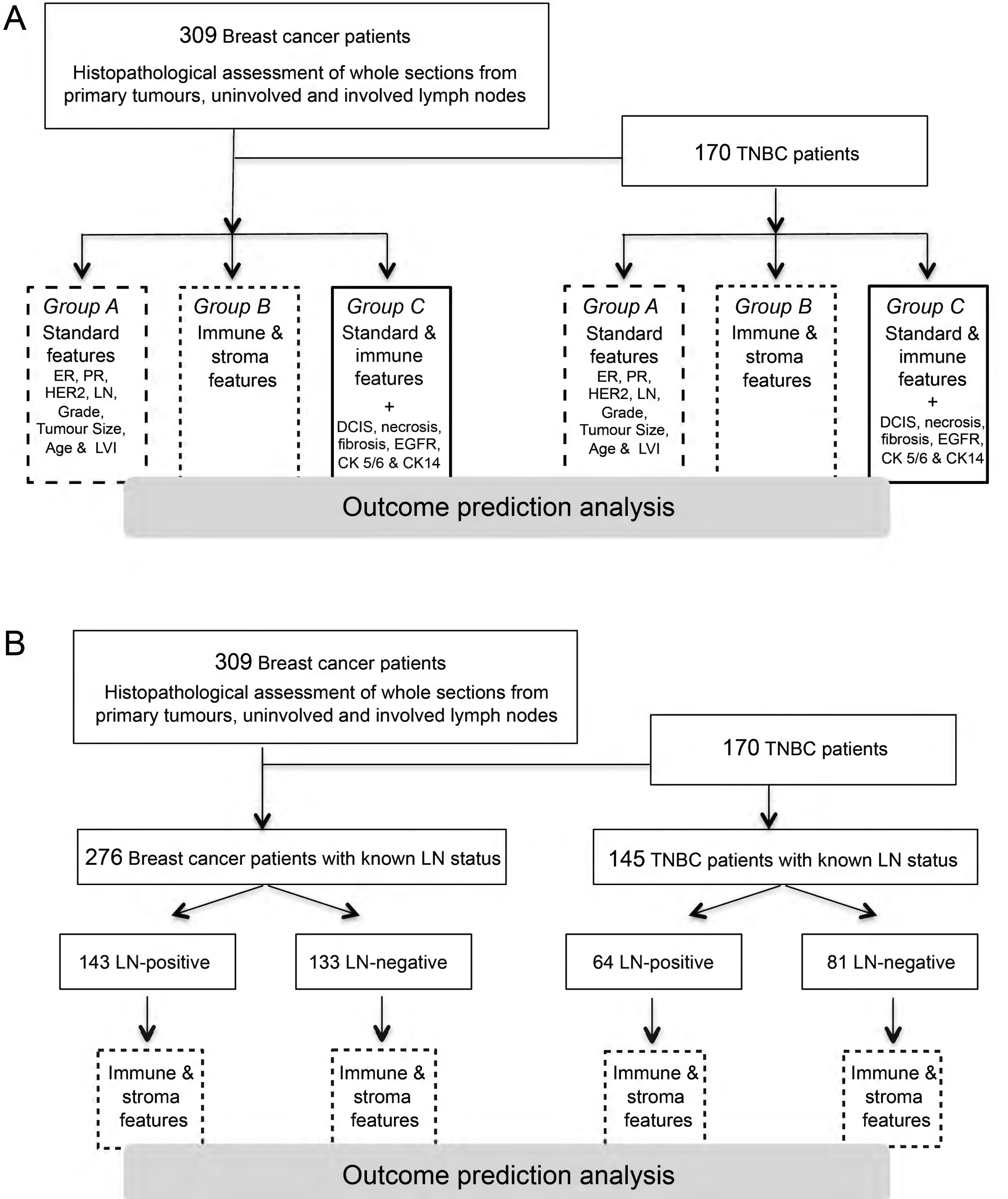
A
309 Breast cancer patients
Histopathological assessment of whole sections from primary tumours, uninvolved and involved lymph nodes
170 TNBC patients
Group A
Standard features
ER, PR, HER2, LN, Grade, Tumour Size, Age & LVI
Group B
Immune & stroma features
Group C
Standard & immune features
+
DCIS, necrosis, fibrosis, EGFR, CK 5/6 & CK14
Group A
Standard features
ER, PR, HER2, LN, Grade, Tumour Size, Age & LVI
Group B
Immune & stroma features
Group C
Standard & immune features
+
DCIS, necrosis, fibrosis, EGFR, CK 5/6 & CK14
Outcome prediction analysis
B
309 Breast cancer patients
Histopathological assessment of whole sections from primary tumours, uninvolved and involved lymph nodes
170 TNBC patients
276 Breast cancer patients with known LN status
145 TNBC patients with known LN status
143 LN-positive
133 LN-negative
64 LN-positive
81 LN-negative
Immune & stroma features
Immune & stroma features
Immune & stroma features
Immune & stroma features
Outcome prediction analysis

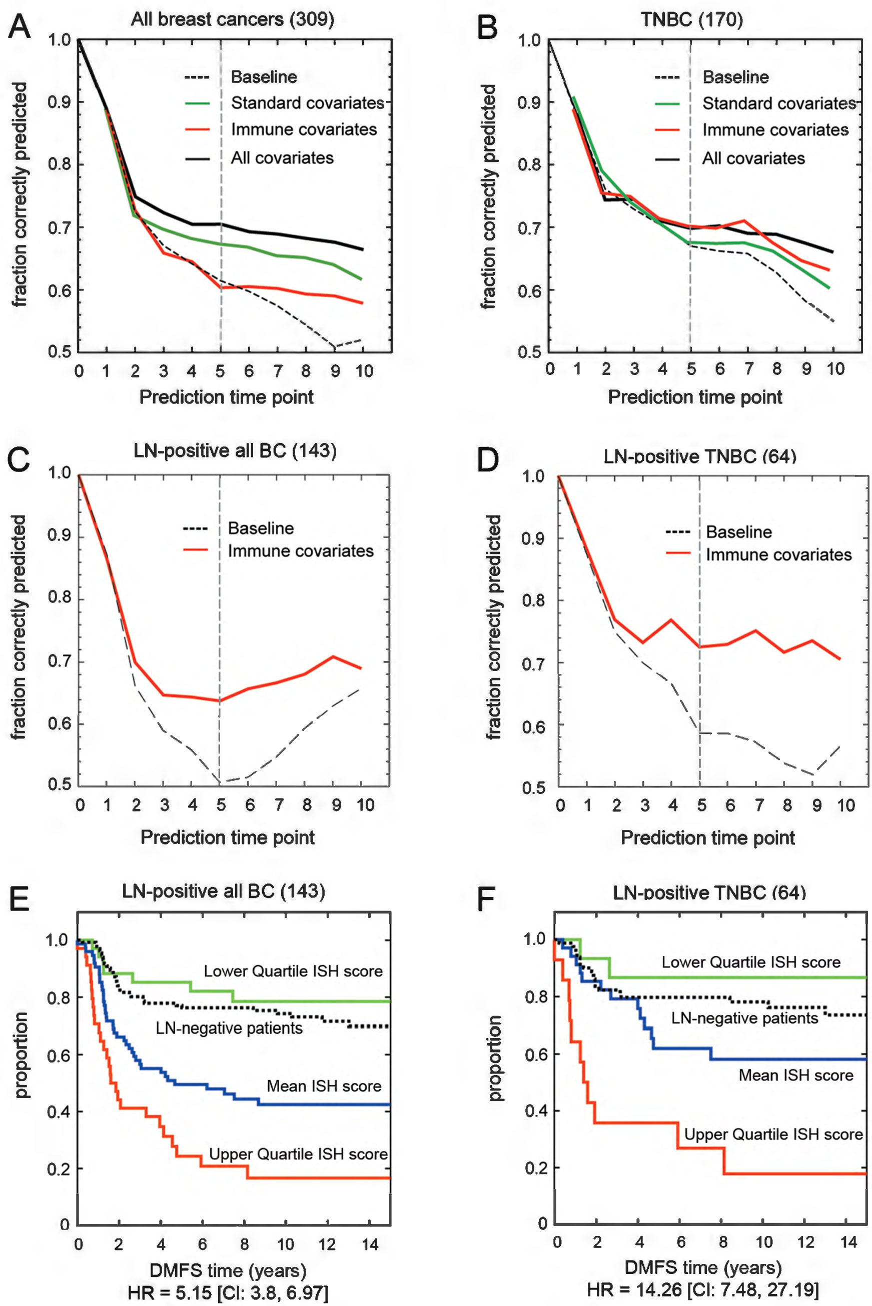
A
All breast cancers (309)
B
TNBC (170)
Baseline
Standard covariates
Immune covariates
All covariates
fraction correctly predicted
Prediction time point
C
LN-positive all BC (143)
D
LN-positive TNBC (64)
Baseline
Immune covariates
fraction correctly predicted
Prediction time point
E
LN-positive all BC (143)
Lower Quartile ISH score
LN-negative patients
Mean ISH score
Upper Quartile ISH score
proportion
DMFS time (years)
HR = 5.15 [CI: 3.8, 6.97]
F
LN-positive TNBC (64)
Lower Quartile ISH score
LN-negative patients
Mean ISH score
Upper Quartile ISH score
proportion
DMFS time (years)
HR = 14.26 [CI: 7.48, 27.19]

Table 2

A Intratumoural and peritumoural assessment

Characteristics assessed	TNBC	Non-TNBC	
	N= 170 (%)	N= 139 (%)	P Value
Semi-quantitative assessment of lymphocytic infiltration across entire tumour			
Absence of lymphocytes	6 (3.5)	18 (12.9)	
Minimal (1-<10%)	18 (10.6)	45 (32.4)	
Mild (10-20%)	45 (26.5)	36 (25.9)	
Moderate (>20-<50%)	78 (45.9)	35 (25.2)	Chi-square-test
Strong (≥50%)	23 (13.5)	5 (3.6)	6.94E-09
TILs scattered in the intratumoural stroma			
Absence of lymphocytes	14 (8.2)	32 (23)	
Minimal (1-<10%)	43 (25.3)	60 (43.2)	
Mild (10-20%)	50 (29.4)	24 (17.3)	
Moderate (>20-<50%)	55 (32.4)	22 (15.8)	Fisher's exact-test
Strong (≥50%)	8 (4.7)	1 (0.7)	1.86E-07
TILs around tumour cell nests			
Absence of lymphocytes	41 (24.1)	61 (43.9)	
Minimal (1-<10%)	33 (19.4)	35 (25.2)	
Mild (10-20%)	29 (17.1)	14 (10.1)	
Moderate (>20-<50%)	55 (32.4)	24 (17.3)	Chi-square-test
Strong (≥50%)	12 (7.1)	5 (3.6)	2.68E-04
TILs at the invasive margin			
Absence of lymphocytes	12 (7.1)	40 (28.8)	
Minimal (1-<10%)	21 (12.4)	33 (23.7)	
Mild (10-20%)	44 (25.9)	33 (23.7)	
Moderate (>20-<50%)	71 (41.8)	31 (22.3)	Chi-square-test
Strong (≥50%)	22 (12.9)	2 (1.4)	5.70E-10
Intratumoural TILs			
Absent	119 (70)	129 (92.8)	Chi-square-test
Present	51 (30)	10 (7.2)	1.14E-06
Lymphocytic infiltrate surrounding DCIS			
DCIS absent	108 (63.5)	71 (51.1)	
Absent	21 (33.9)	27 (39.7)	
Mild (10-20%)	11 (17.7)	17 (25)	
Moderate (>20-<50%)	14 (22.6)	8 (11.8)	Chi-square-test
Strong (≥50%)	16 (25.8)	16 (23.5)	8.14E-02
Salgado's classification			
0-10% stromal TILs	39 (22.9)	77 (55.4)	
20-40% stromal TILs	61 (35.9)	37 (26.6)	Chi-square-test
50-90% stromal TILs	70 (41.2)	25 (17.9)	9.70E-09
TILs surrounding normal breast lobules			
No normal breast lobules	39 (22.9)	25 (17.9)	
Normal breast lobules			
Absent	26 (19.8)	35 (30.7)	
Mild (10-20%)	30 (22.9)	34 (29.8)	
Moderate (>20-<50%)	35 (26.7)	25 (21.9)	Chi-square-test
Strong (≥50%)	40 (30.5)	20 (17.5)	3.25E-02
Perivascular infiltrate			
Absent	28 (16.5)	22 (15.8)	
Mild (10-20%)	52 (30.6)	50 (35.9)	
Moderate (>20-<50%)	53 (31.2)	37 (26.6)	Chi-square-test
Strong (≥50%)	37 (21.8)	30 (21.6)	7.44E-01
Lymphocytic lobulitis			
No normal breast lobules	39 (22.9)	25 (17.9)	
Absent	110 (83)	103 (90.4)	Chi-square-test
Present	21 (16)	11 (9.6)	1.88E-01
Tertiary lymphoid structures			
Absent	123 (72.4)	115 (82.7)	Chi-square-test
Present	47 (27.6)	24 (17.3)	4.32E-02

B Stromal features

Characteristics assessed	TNBC	Non-TNBC	
	N= 170 (%)	N= 139 (%)	P Value
Oedemamtous/Myxoid stroma			
Absent	125 (73.5)	114 (82)	
Present	41 (24.1)	25 (18)	Fisher's exact-test
Dominant	4 (2.4)	0 (0)	6.79E-02
Hyalinised stroma			
Absent	21 (12.4)	21 (15.1)	
Present	129 (75.9)	103 (74.1)	Chi-square-test
Dominant	20 (11.8)	15 (10.8)	7.70E-01
Fibroblastic stroma			
Absent	20 (11.8)	20 (14.4)	
Present	137 (80.6)	110 (79.1)	Chi-square-test
Dominant	13 (7.6)	9 (6.5)	7.50E-01

C Lymph node

	LN-Positive Patients		LN-Negative Patients
Characteristics assessed	Involved LN	Uninvolved LN	Uninvolved LN
	N=143 (%)	N=143 (%)	N= 133 (%)
Germinal Centre (GC) assessable	97 (67.8)	88 (61.5)	105 (78.9)
Complete absence of GC	26 (18.2)	46 (32.2)	28 (21.1)
Total metastatic replacement of LN	20 (14)	NA	NA
No uninvolved LN available for assessment	NA	9 (6.3)	NA
GC semi-quantitative assessment			
Grade 1 (Few)	37 (38.1)	34 (38.6)	45 (42.9)
Grade 2 (Moderate)	41 (42.3)	31 (35.2)	29 (27.6)
Grade 3 (Numerous)	19 (19.6)	23 (26.1)	31 (29.5)
GC location			
Peripheral	51 (52.6)	34 (38.6)	50 (47.6)
Predominantly peripheral	19 (19.6)	27 (30.7)	23 (21.9)
Central	6 (6.2)	0 (0)	0 (0)
Predominantly central	21 (21.6)	27 (30.7)	32 (30.5)
GC size			
Small	23 (23.7)	20 (22.7)	32 (30.5)
Moderate	13 (13.4)	11 (12.5)	14 (13.3)
Large	4 (4.1)	4 (4.5)	4 (3.8)
Mixed	57 (58.8)	53 (60.2)	55 (52.4)
GC hyperplasia			
Absent	52 (53.6)	48 (54.5)	65 (61.9)
Present	45 (46.4)	40 (45.5)	40 (38.1)
Sinus histocytosis			
Grade 1 = <2 cells across	1 (1.1)	3 (2.2)	3 (2.3)
Grade 2 = 2 to 4	9 (9.5)	24 (17.9)	14 (10.5)
Grade 3 = >4 to <8	41 (43.2)	50 (37.3)	61 (45.9)
Grade 4 = ≥8	44 (46.3)	57 (42.5)	55 (41.4)
No uninvolved LN available for assessment	NA	9	NA
SH Mets Replacement	48	NA	NA
Metastatic pattern			
Subcapsular	4 (2.8)	NA	NA
Sinusoidal	7 (4.9)	NA	NA
Diffuse	6 (4.2)	NA	NA
Nodular	45 (31.5)	NA	NA
Mixed	61 (42.7)	NA	NA
Total metastatic replacement of LN	20 (14)	NA	NA

Table 1

Clinicopathological features	All Breast Cancers N=309 (%)	TNBC N=170 (%)
Age at diagnosis		
<Below 50 years	106 (34)	61 (36)
Over 50 years	203 (66)	109 (64)
Tumor size, cm		
pT1	68 (22)	35 (21)
pT2	183 (59)	103 (61)
pT3	45 (15)	26 (15)
Unknown	13 (4)	7 (4)
Histological grade		
I	9 (3)	1 (0.5)
II	47 (15)	7 (4)
III	253 (82)	162 (95.5)
Histological subtypes		
Invasive breast carcinoma of no special type	253 (81)	143 (84)
Mixed ductal and lobular carcinoma	24 (8)	10 (5.8)
Invasive lobular carcinoma	11 (4)	5 (2.9)
Carcinoma with apocrine differentiation	9 (3)	2 (1.2)
Metaplastic carcinoma of no special type	4 (1)	4 (2.4)
Invasive papillary carcinoma	2 (0.6)	2 (1.2)
Carcinoma with medullary features	2 (0.6)	2 (1.2)
Salivary gland / skin adnexal type tumors	2 (0.6)	2 (1.2)
Adenosquamous carcinoma	1 (0.3)	0
Secretory carcinoma	1 (0.3)	0
DCIS		
Present	143 (46)	66 (39)
Absent	163 (53)	102 (60)
Unknown	3 (1)	2 (1)
Necrosis		
Present	106 (34)	61 (36)
Absent	203 (66)	109 (64)
Fibrosis		
Present	90 (29)	54 (36)
Absent	216 (70)	115 (64)
Unknown	3 (1)	1 (0.5)
Lymphovascular invasion		
Present	90 (29)	45 (26)
Absent	216 (70)	124 (73)
Unknown	3 (1)	1 (0.5)
Lymph node status		
Positive	143 (46)	64 (38)
Negative	133 (43)	81 (47)
Unknown	33 (11)	25 (15)
Distant Metastasis		
Present	129 (42)	59 (35)
Absent	180 (58)	111 (65)
Immunohistochemical subtypes		
Hormone receptor+ /HER2-	62 (20)	NA
Hormone receptor-/HER2+	59 (19)	NA
Hormone receptor+/HER2+	18 (6)	NA
Triple Negative	170 (55)	170 (100)
EGFR		
Present	67 (22)	53 (31)
Absent	225 (73)	106 (63)
Unknown	17 (5)	11 (7)
CK5/6		
Present	68 (22)	57 (3)
Absent	225 (73)	103 (61)
Unknown	16 (5)	10 (6)
CK14		
Present	49 (16)	44 (26)
Absent	244 (79)	114 (67)
Unknown	16 (5)	12 (7)

Table 3
Feature selection from multivariate Bayesian Cox regression analyses

	LN-positive and LN-negative						LN-positive		LN-negative	
	All breast cancers			TNBC			All breast cancers	TNBC	All breast cancers	TNBC
Selected features to predict risk for developing distant metastasis	Group A	Group B	Group C	Group A	Group B	Group C	Group B	Group B	Group B	Group B
	Standard	Immune & stroma	All features	Standard	Immune & stroma	All features	Immune & stroma	Immune & stroma	Immune & stroma	Immune & stroma
LN-status	1.904		2.248	1.558		1.635				
ER-status			0.7							
HER2-status	1.797		1.76							
LVI-status	1.483			1.642						
Fibrosis			1.55							
Salgado's classification		0.67	0.629				0.687	0.282		
TILs at the invasive margin			0.509			0.571	0.487			
Lmyphocytic lobulitis					0.368	0.436	0.591	0.339		0.196
Lymphoid infiltrate surrounding DCIS						0.358				
Tertiary lymphoid structures						2.298				2.24
Oedematous/Myxoid stroma						1.889			2.22	3.32
Germinal centre, semi-quantitative assessment in uninvolved LN		0.348	0.248		0.413	0.451	0.212	0.11		
Germinal centre, semi-quantitative assessment in involved LN		0.541	0.654			0.496				0.426
Germinal centre, size in uninvolved LN		2.216	2.071				2.659	2.713		
Germinal centre, size in involved LN						3.504				
Germinal centre, location in involved LN		2.932	3.04		3.401	3.758	2.234	2.898		
Germinal centre, hyperplasia in uninvolved LN			1.59							
Germinal centre, hyperplasia in involved LN					0.371	0.278		0.666		
Metastatic pattern in involved LN					2.221	4.11		3.334		

Supplementary Figure S1. Exemplars of stromal tissue stained with smooth muscle actin and Alcian blue.A. Oedematous/myxoid stroma with characteristically vacuolated material admixed with collagen fibres; **B.** fibroblastic stroma with numerous stromal cells (fibroblasts); **C.** hyalinised stroma. Figures show tissue stained with H&E; Smooth Muscle Actin (SMA) (Dako Ab Cat. #0851, antibody used at 1:200 concentration, antigen retrieval performed with 18min microwaving in citric buffer pH6.); and Alcian blue staining (Alcian blue 8GX, Generon).

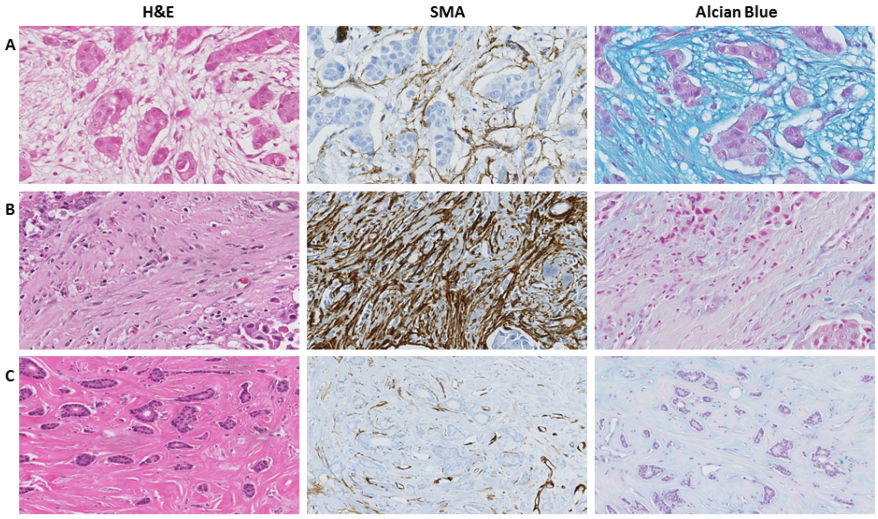

Quantification of SMA with HistoQuest. A. oedematous/myxoid stroma; **B.** fibroblastic stroma; **C.** hyalinised stroma.

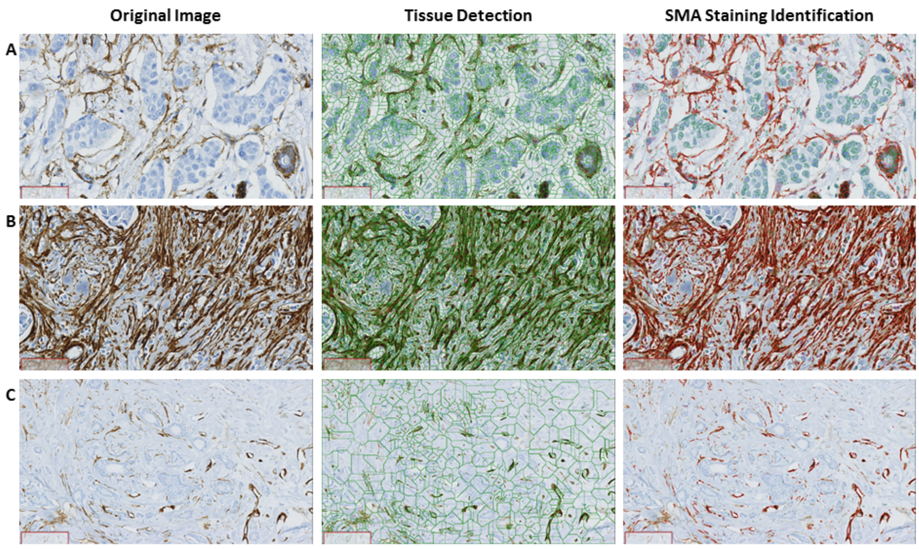

Histograms of DAB stained surface areas in μm2.

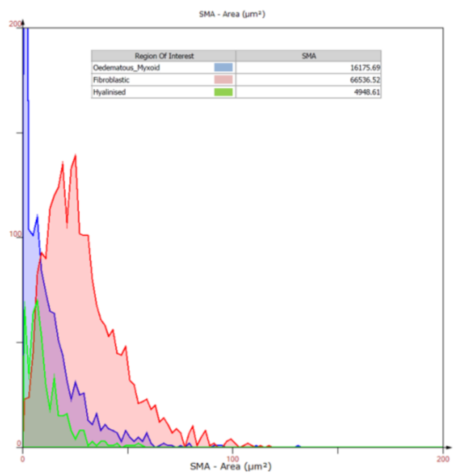

Supplementary Figure S2

I A. Lymph node with predominantly primary follicles (H&E); **B.** Lymph node with predominantly primary follicles (CD20); **C.** Lymph node with secondary follicles with germinal centres and sinus histiocytosis (H&E); **D.** Lymph node with secondary follicles with germinal centres (CD20).

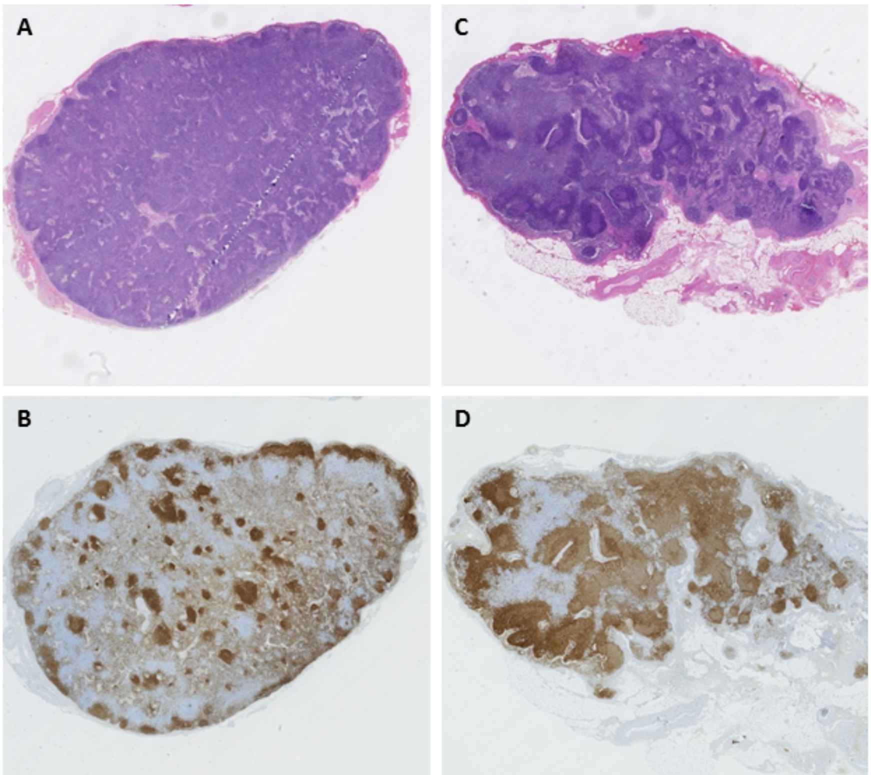

II A. Primary follicles; **B.** Germinal centre; Tissue stained with a B cell marker CD20 [Dako Cat. #7019, citrate buffer, 1:50 dilution] and a dendritic cell marker CD11c [Abcam Cat. #52631, citrate buffer, 1:100 dilution].

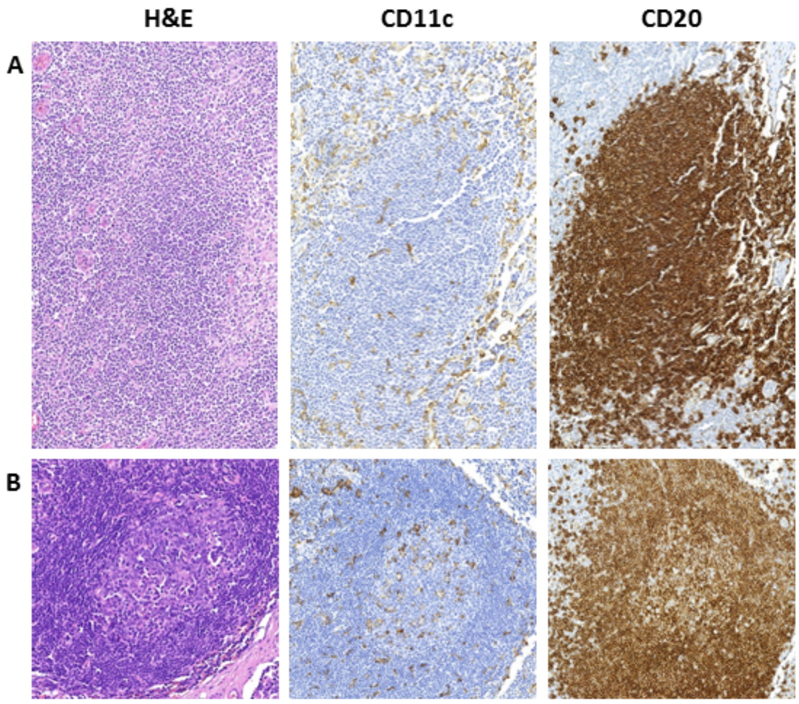

Supplementary Figure S4

A **All covariate in breast cancers**

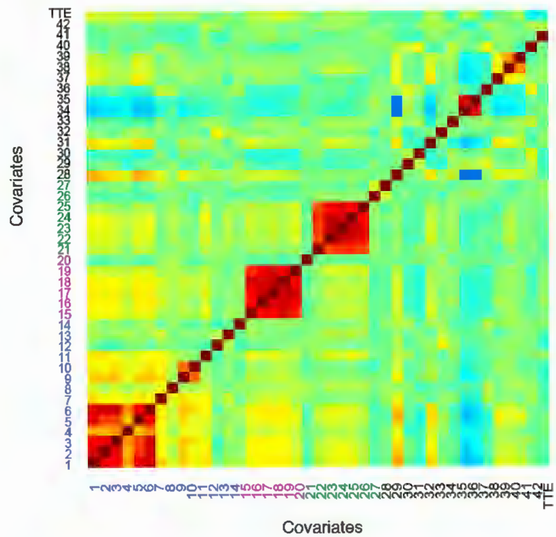

B **Immune features in TNBC**

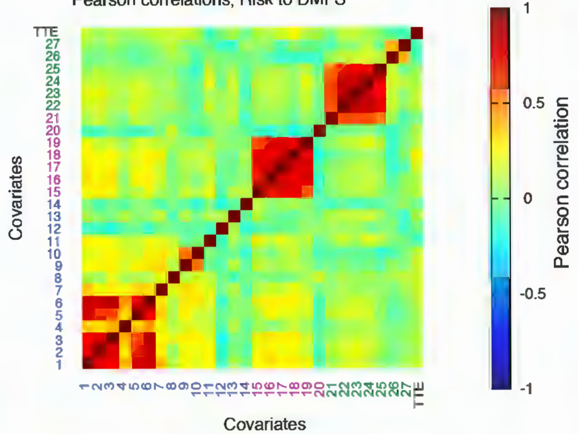

	Covariate		Covariate		Covariate
1	Semi-quantitative scoring of TILs	15	Uninvolved LN: Germinal centre- location	28	Histological Grade
2	TILs in stromal compartment	16	Uninvolved LN:Germinal centre-size	29	DCIS at invasive tumour
3	TILs around tumour cell nests	17	Uninvolved LN:Germinal centre-large siz	30	LVI
4	TILs within tumour cell nests	18	Uninvolved LN:Germinal centre -number	31	Necrosis
5	Tumour edge associated TILs invasive front	19	Uninvolved LN:Germinal centre present	32	Fibrosis
6	Salgado 'Mimic'	20	Uninvolved LN: Sinus histocytosis	33	Pathological subtypes
7	TILs surrounding DCIS	21	Involved LN: Germinal centre- location	34	ER IHC
8	Perivascular lymphoid cells	22	Involved LN:Germinal centre- size	35	PR IHC
9	Dense nests of TILs at normal breast lobules	23	Involved LN:Germinal centre - large size	36	HER2 IHC
10	Lymphocytic lobulitis	24	Involved LN:Germinal centre - number	37	EGFR IHC
11	Ectopic lymph node-like structures	25	Involved LN:Germinal centre present	38	CK5/6 IHC
12	Oedematous/Myxoid	26	Involved LN: Sinus histocytosis	39	CK14 IHC
13	Hyalinised Stroma	27	Involved LN: Metastatic pattern	40	Lymph Node Status
14	Fibroblastic Stroma			41	Age at diagnosis
				42	Tumour size categorical

Supplementary Figure S5

LN-negative

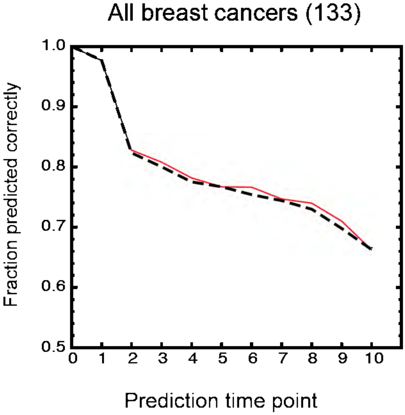

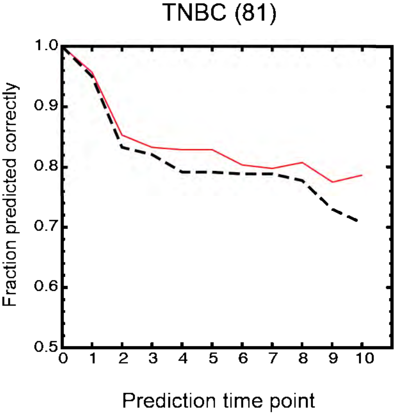

Supplementary Figure S3: Identification of overfitting point in the Bayesian batch Cox analysis. Graphs illustrating the fraction of correctly predicted disease outcome for patients (i.e. those who had an event prior the cut-off time) (prediction time point) over those patients who had either never distant metastasis or developed metastasis after this time point. The top and bottom lines represent the validation and test sets, respectively. The number of covariates used for the prediction is shown on the x-axis (*nr of covs*). Iteratively, covariates are removed from the analysis.